J Solid State Electrochem (2006) 10:785–791
DOI 10.1007/s10008-006-0169-0

ORIGINAL PAPER

An examination of the conditions resulting in a temporal convolution related to electrochemical processes

Peter J. Mahon · Keith B. Oldham

Received: 13 April 2006 / Revised: 24 April 2006 / Accepted: 2 May 2006 / Published online: 7 June 2006

Abstract Temporal convolutions represent an important subset for the description of electrochemical systems and enable powerful simplifications to be employed during the analysis of experimental data. However, the circumstances amenable to the acquisition of suitable experimental data are restricted and previously proposed conditions based on concepts that relate to uniform concentration distributions at electrode surfaces are further demonstrated based on the analysis of a hybrid electrode geometry.

Keywords Convolution · Electrode Geometry · Uniform Flux · Uniform Accessibility · Cyclic Voltammetry

Introduction

Almost all (or perhaps all) analytical treatments of voltammetric processes treat conditions on the electrode surface, such as surface concentrations, as spatially uniform. Why is this so? Because, when surface concentrations are not uniform, the flux of the substrate arriving at the electrode will not be at right-angles to the surface. This, in itself, is not a problem, but its consequence is that the route by which the substrate reaches the electrode will change with time and this circumstance is one that is very difficult to treat analytically. You can treat such processes by digital simulation (by finite element modeling, especially) and this is the way to go in modeling experiments that result in non-uniform surface concentrations. So what are the consequences for the analytical modeler of voltammetry with the restriction to uniform surface concentrations? What voltammetric conditions lead to the uniform surface concentrations?

Until fairly recently, semi-infinite voltammetric phenomena have been generally considered under predominantly planar diffusion conditions with the electrode curvature and edge effects being thought of as distortions that could be overcome by applying appropriate corrections [1–11]. However, with the advent of microelectrodes and their large variety of geometries, a widening area of research has developed in an effort to exploit the great practical advantages that reducing at least one of the electrode's spatial dimensions enables [6]. The subsequent decrease in exposed surface area, and thereby current, minimizes difficulties with regard to potential control and reduces the capacitive contribution of the electrode [6, 12–15]. On the basis of geometric considerations, reducing the size of the electrode in two dimensions proves to be even better for discriminating against these interferences because it may be possible to obtain true steady-state behavior [16, 17]. These benefits are generally weighed against a significant decrease in the magnitude of the current, which has its own inherent problems and in some cases this has been overcome by the use of electrode arrays [6, 18–21].

Vieil, both independently [22, 23] and with others [24–26], has demonstrated great insight into the understanding of a generalized approach to indeterminate transport and electrode geometry situations. This body of work showed that by measuring the current under con-

Submitted in recognition of the contributions to chemistry of Alan M. Bond, a brilliant scientist and a generous mentor, colleague and friend, on the occasion of his sixtieth birthday.

P. J. Mahon (✉)
Research School of Chemistry, Australian National University,
Canberra, ACT 0200, Australia
e-mail: mahon@rsc.anu.edu.au

K. B. Oldham
Department of Chemistry, Trent University,
Peterborough, ON K9J 7B8, Canada

ditions that were transport limited, it is possible to apply convolution procedures to eliminate effects due to electrode geometry and poorly defined transport. We will explore this implication in some depth throughout this paper.

In general, we will consider the following electrochemical reaction in which a solution soluble substrate, S, diffuses to an electrode surface and is reduced or oxidized to produce a product, P, which then diffuses away from the electrode.

$$S_{soln} - ne^- \leftrightarrows P_{soln} \quad (1)$$

The number of electrons transferred between electrode and substrate is given by n, an integer of either sign and in accordance with the IUPAC convention, having the same sign as the current. Further complications due to the chemical stability of the product will also be considered.

The rigorous mathematical analysis of this electrochemical system, with diffusion being the only mode of transport, requires the solution of Fick's second law pursuant to the initial and remote boundary conditions of each unique situation. Often this treatment results in a solution where the time-dependent current and the respective concentrations of the substrate and product at an electrode surface are related via a convolution with a third time-dependent function. These systems represent an important subset of all electrochemical systems because major simplifications are possible from a theoretical perspective due to the elimination of spatial inhomogeneity at the electrode surface.

In fact, two separate but related convolutions have been identified [27–30]

$$c_S^s(t) = c_S^b - \frac{I(t)*g(t)}{nFA\sqrt{D}} \quad (2)$$

$$I(t) = nFA\sqrt{D}\frac{d\Delta c_S(t)}{dt}*h(t) \quad (3)$$

where $I(t)$ is the current, $\Delta c_S(t) = c_S^b - c_S^s(t)$, c_S^b is the substrate concentration in the bulk solution, $c_S^s(t)$ is the substrate concentration at the electrode surface, F is Faraday's constant, A is the electrode area and D is the diffusivity.[1] The remaining time-dependent functions $g(t)$ and $h(t)$ have been shown to be also dependent upon electrode geometry and rate constants, if homogeneous kinetics are involved [27, 29]. Functions $g(t)$ and $h(t)$ are interrelated and have been described as conjugate functions [27, 29], they each have a dimensionality corresponding to the $s^{-1/2}$ unit. The asterisk represents the shorthand notation for the convolution operation [31] and has the same dimension as time. The utility of equations (2) and (3) have been demonstrated in the direct analysis of voltammetric data whereby transport, thermodynamic and kinetic parameters have been quantified [24–27, 32, 33]. Modeling applications describing both controlled potential and controlled current experiments have also been presented [24, 27–30, 34].

It has been demonstrated that Eq. (2), developed in the context of the extended semiintegral, is a generalized form that incorporates Fick's laws [34]. Uniformity of concentration across the electrode surface was proposed to be the requirement for the voltammetry to be describable by a temporal convolution integral. Three circumstances were proposed under which this might occur [29, 34]. The first case involves an electrode that is geometrically *uniformly accessible*; that is an electrode where symmetry dictates that the rate of transport be equal at all points on the surface. When the current is limited by the rate of transport a uniform concentration distribution will result at the electrode surface when the initial concentration distribution is uniform and this is the situation in most electrochemical experiments. In practice, the only such geometries are a suitably shrouded (or very large) plane, a capped cylinder, an isolated sphere or a sessile hemisphere. Secondly, if the electrochemical reaction is reversible then the uniformity of the potential and Nernst's law conspire to ensure that the ratio of activities for the substrate and product is also uniform across the electrode surface. The third situation is when the polarization is so intense that the concentration of the substrate at the electrode surface is virtually zero, this will lead to a uniform distribution of the product across the electrode surface even if the reaction is not reversible. In this case, conservation laws ensure that the product is generated uniformly.

The emergence of various modeling and analysis schemes which are based upon the convolution of two time-dependent functions must therefore be restricted to situations where one of the previously outlined three cases can be clearly identified. The proposed framework enables cases to be identified so that experimental conditions may be selected that provide for simplifying interpretation without the need to rigorously derive the full mathematical solution.

Previously [29], we briefly considered a hybrid electrode based on the combination of two isolated hemispheres but the large disparity in the area of the two hemispheres caused the larger electrode to dominate the smaller electrode when interpretations based on the current (or a functions proportional to the current) were considered. In this paper, we will examine each of the three proposed conditions by exploring the properties of a hybrid electrode that is a combination of hemispherical electrodes where tractable theoretical solutions exist.

[1] or diffusion coefficient

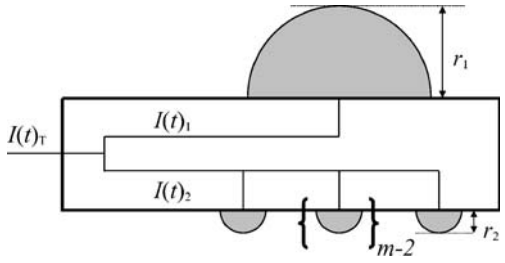

Fig. 1 A diagram of the hybrid electrode

Analysis of the hybrid electrode

In order to examine the three circumstances and identify whether other conditions exist which may result in a uniform surface concentration across the electrode surface, it is necessary to consider an electrode that may not be uniformly accessible in all circumstances but has a tractable analytical solution for many electrode kinetic conditions. Figure 1 is a diagram of an electrode that satisfies these requirements.

The electrode is a combination of two hemispherical geometries of different radii. The area of the larger hemisphere of radius r_1 is adjusted so that it has the same surface area as the number of smaller hemispheres, m, of radius r_2. This ensures that the exposed electrode area is equal for both sides of the insulating support. A distance that ensures that they are diffusionally isolated from each other separates the smaller hemispheres from each other and from the large hemisphere. Both sides of the support can be considered separately and the current for the smaller hemispheres is summed to be equal to $I(t)_2$. The total current, $I(t)_T$, will be the sum of $I(t)_1$ and $I(t)_2$.

It is envisaged that the size of the large hemisphere on one side could ensure predominantly transient diffusion at that part of the electrode surface while the large number of small hemispheres on the other side might experience almost steady-state diffusion on the same time scale. In this way significant variations in substrate flux can be observed independently of the uniformity of the substrate concentration.

Transport limited case

In a potential-step experiment in which a severe overpotential is applied such that the potential is in the transport-limited region, then Eq. (3) simplifies because the surface concentration of the substrate is effectively zero and the convolution integral devolves into a multiplication.

$$I(t) = nFA\sqrt{D}c_S^b h(t) \tag{4}$$

It follows that there is a straightforward relationship between the transport function $h(t)$ and the observed limiting current. In this way it is possible experimentally to obtain knowledge of the transport characteristics of the electrochemical system [22–26, 29].

In general, the equation for the transport limited current at a spherical electrode of radius, r, is given by [29]

$$I(t) = nFA\sqrt{D}c_S^b\left[\frac{1}{\sqrt{\pi t}} + \frac{\sqrt{D}}{r}\right] \tag{5}$$

The individual currents for each of the differently sized hemispheres for the hybrid electrode are

$$I(t)_1 = nFA_1\sqrt{D}c_S^b\left[\frac{1}{\sqrt{\pi t}} + \frac{\sqrt{D}}{r_1}\right] \tag{6}$$

$$I(t)_2 = nFmA_2\sqrt{D}c_S^b\left[\frac{1}{\sqrt{\pi t}} + \frac{\sqrt{D}}{r_2}\right] \tag{7}$$

where A_1 is the area of the hemispherical electrode with a radius of r_1, A_2 is the area of the hemispherical electrode with a radius of r_2 and overall $A_1 = mA_2$.

For the hybrid electrode of Fig. 1, the total current is

$$I(t)_T = I(t)_1 + I(t)_2 = nFA_T\sqrt{D}c_S^b\left[\frac{1}{\sqrt{\pi t}} + \frac{\sqrt{D}(r_1 + r_2)}{2r_1r_2}\right] \tag{8}$$

where $A_T = A_1 + mA_2$. Due to the equal electrode surface area on each side of the insulator, it follows that Eq. (8) simplifies to be of the same form as Eq. (5)

$$I(t)_{Tesm} = nFA_T\sqrt{D}c_S^b\left[\frac{1}{\sqrt{\pi t}} + \frac{\sqrt{D}}{r_{esm}}\right] \tag{9}$$

when the following definitions are made on the basis that $A_1 = mA_2$

$$r_{esm} = \frac{2r_1r_2}{r_1 + r_2} = \frac{2r_1}{1 + \sqrt{m}} = \frac{2\sqrt{m}r_2}{1 + \sqrt{m}} \tag{10}$$

and Eq. (9) states that the hybrid electrode has an area of a sphere with radius r_1 (or $\sqrt{m}r_2$) but has a *sphericity* equivalent to a radius of r_{esm} that is somewhere between r_1 and r_2 depending on the value of m. We will refer to this as the *equivalent sphericity model* (*esm*).[2] The transport limited, geometry dependent function $h(t)_{Tesm}$ for the hybrid electrode is

$$h(t)_{Tesm} = \frac{1}{\sqrt{\pi t}} + \frac{\sqrt{D}}{r_{esm}} \tag{11}$$

and further modeling and analysis applications involving Eq. (11) are possible for this specific electrode geometry.

[2] An initial observation is that when $m = 1$ (i.e. $r_1 = r_2 = r_{esm}$), the hybrid electrode behaves as if it were a simple sphere that is geometrically "uniformly accessible". At this limit it is well-established that a temporal convolution occurs.

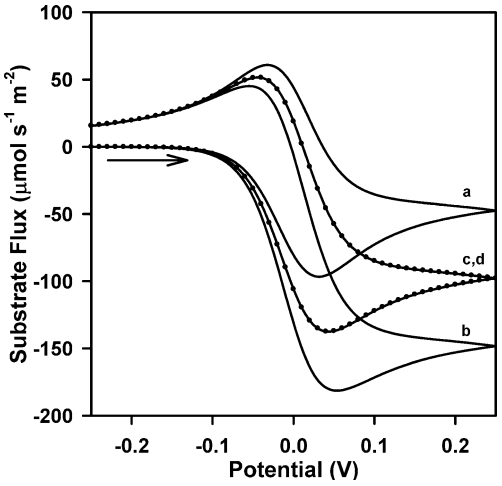

Fig. 2 A plot of the substrate fluxes for the reversible electron transfer case. The curves are (a) $-I(t)_1/nFA_1$ and (b) $-I(t)_2/nFmA_2$ (c) $-I(t)_T/nFA_T$ and (d) $-I(t)_{Tesm}/nFA_T$ (••••). The geometric parameters are r_1=8.921×10^{-5} m, r_2=8.921×10^{-6} m, r_{ecm}=1.622×10^{-5} m and m=100. Other parameters are: scan rate=1 V s^{-1}, D=1×10^{-9} m^2 s^{-1} and c_S^b=1 mM

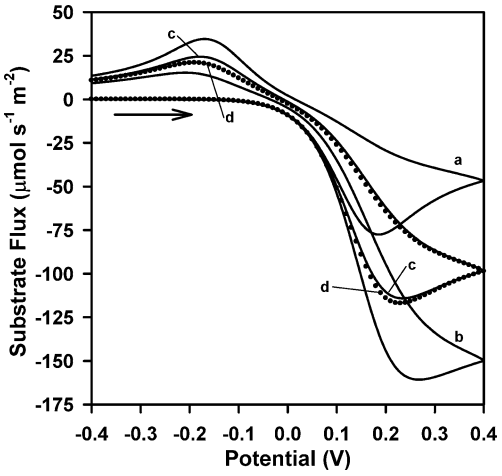

Fig. 4 The substrate fluxes for the quasi-reversible electron transfer case with parameters as given in Fig. 2 but with a heterogeneous rate constant, k^o=1×10^{-5} m s^{-1}

Both convolutive modeling [27, 29] and finite-difference digital simulations using Digisim [35] were used to simulate a series of cyclic voltammograms. Spherical electrode geometry was employed to simulate the two different hemispheres of the hybrid electrode and the current for the number of smaller hemispheres was summed to obtain $I_2(t)$. The current for the *equivalent sphericity model* was calculated on the basis of the equivalent radius calculated from Eq. (10) and the current was then multiplied by an area ratio factor to obtain the expected current. No difference between the two simulation methods was observed. Substrate fluxes at the electrode surface (i.e. $-I(t)/nFA$) were derived from these currents and surface concentrations were simultaneously derived from the simulations.

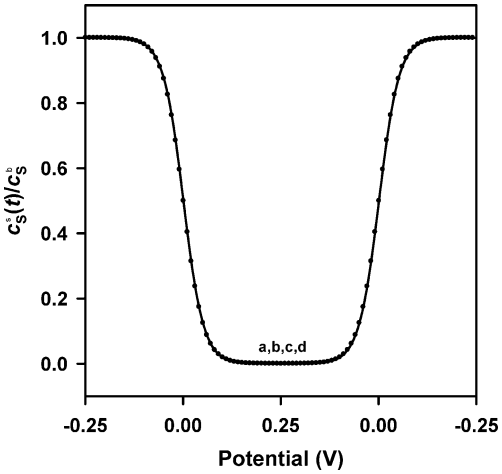

Fig. 3 The surface concentrations for the reversible electron transfer case. Parameters are as given in Fig. 2

The nernstian or reversible case

By way of demonstration, Fig. 2 reports substrate fluxes derived from simulated cyclic voltammograms and the diagram contains curves describing four geometric conditions. Curve (c) was obtained by summing all the individual current contributions from the hybrid electrode whereas curve (d) is based on an electrode of radius, r_{esm}. As expected from the previous discussion there is no difference between the two superimposed curves in this diagram. The remaining curves display the separate substrate fluxes from each side of the hybrid electrode and the greater flux at the smaller dimensioned hemispheres can be observed as curve (b). Figure 3 is a plot of the substrate surface concentration under reversible conditions for the four situations (i.e. either side of the hybrid electrode, the average surface concentration for the hybrid electrode and for the *esm*) and it is apparent that there is no concentration disparity displayed between any of these curves. The explanation for this is that the surface concentration of the substrate is only dependent upon the applied potential, $E(t)$, as given by the following form of the Nernst equation

$$c_S^s(t) = \frac{1}{1 + exp\left\{\frac{nF}{RT}[E(t) - E^o]\right\}} \tag{12}$$

where E^o is the *standard* or *conditional* potential, R is the gas constant and T is the absolute temperature.

It follows that even though the flux distribution is not uniform for the hybrid electrode, the average flux and the transport limited equivalent are equal. The surface concentration distribution is uniform under reversible conditions and this analysis, along with other examples [30], implies the important concept that the transport for all electrodes can be described by a geometry-specific time-dependent

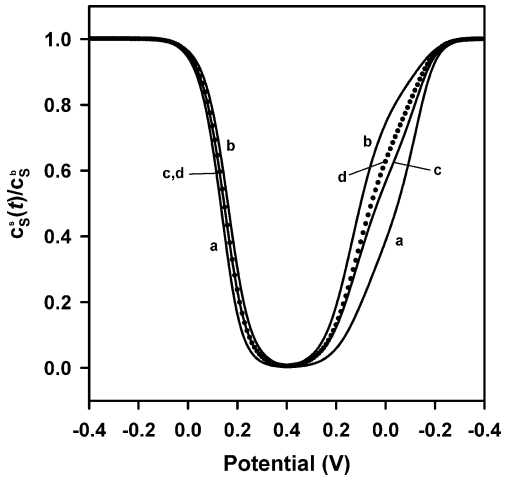

Fig. 5 The surface concentrations for the quasi-reversible electron transfer case with parameters as given in Fig. 4

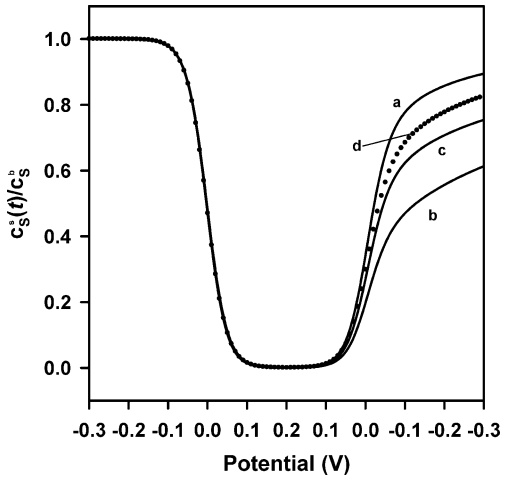

Fig. 7 The surface concentrations for an irreversible chemical reaction with parameters as given in Fig. 6

function when uncomplicated reversible electron transfer is operative. In this way, the second predicted circumstance associated with reversibility is demonstrated.

The quasi-reversible case

If we now consider the quasi-reversible case, the interesting question pertains as to whether the surface concentration and the average substrate flux at the hybrid electrode still correlates with the *esm*. This is investigated in Figs. 4 and 5 where the substrate fluxes and concentrations for the quasi-reversible case are respectively displayed. Significant differences between curves (c) and (d) in both figures are apparent. In this case, both a non-uniform substrate flux and a non-uniform surface concentration distribution occur.

This can be explained if we consider the following equation that relates the potential dependent rates of

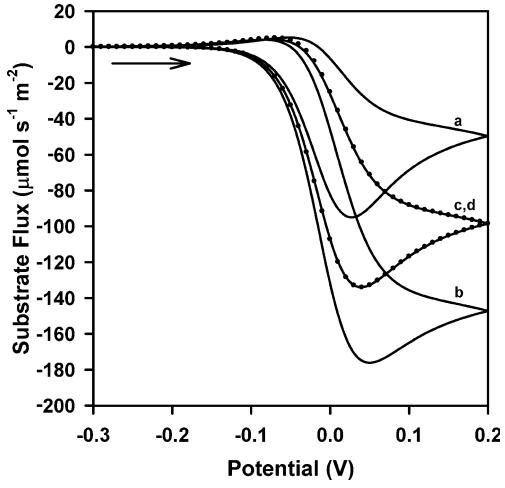

Fig. 6 The substrate fluxes for an irreversible chemical reaction with parameters as given in Fig. 2 but with a first-order rate constant k=10 s^{-1} for the following chemical reaction

electron transfer for the forward, k_f, and backward, k_b, reactions with the current and the surface concentrations of the substrate and the product

$$I(t) = nFA\left(k_f c_S^s(t) - k_b c_P^s(t)\right) \tag{13}$$

If we can assume that the diffusivities of the substrate and product are identical then we can substitute $c_P^s(t) = c_S^b - c_S^s(t)$ and the following general result is obtained.

$$c_S^s(t) = \frac{\frac{I(t)}{nFA} + c_S^b k_b}{k_f + k_b} \tag{14}$$

Without assuming a particular model for the electron transfer, Eq. (14) shows that the surface concentration of the substrate is dependent on the surface flux (i.e. $-I(t)/nFA$). For the substrate at the hybrid electrode, the overall surface concentration will be the average of the surface concentrations for the hemispheres on either side of the support and Fig. 4 shows that these have different surface fluxes depending on the radius of the individual hemispheres. This demonstrates that the surface concentration for *equivalent sphericity model* will only adequately predict the hybrid electrode for the quasi-reversible case if the substrate flux at all points on the electrode surface is equal.

A scenario that would minimize the demonstrated dispersion includes restricting the time domain of the experiment to ensure that the response of the hybrid electrode is dominated by planar diffusion at sufficiently short times (i.e. $-I(t)/nFA$). In general, it would be expected that all electrode geometries could be treated in a similar manner at this limit where the non-planar diffusion component is restricted [36] and this concept has been exploited experimentally on many occasions [37–39].

In this case, it is also noticeable that at potentials in excess of 200 mV from the peak potentials that both the substrate fluxes and concentration distributions merge and

this is a demonstration that at these potentials the third proposed condition based on intense polarization is being satisfied. The following requirement needs to be obtained for this to be the case.

$$k_f + k_b >> \frac{D}{r} \tag{15}$$

Of course, if $k_f + k_b$ is large enough at E° then a reversible situation develops.[3]

The case involving an irreversible chemical reaction

The first-order irreversible homogeneous chemical reaction where P is consumed can also be considered.

$$S_{soln} - ne^- \leftrightarrows P_{soln} \rightarrow Y_{soln} \tag{16}$$

The first-order rate constant, k, describes the formation of Y_{soln}.

Figures 6 and 7 show the effect of a value of k large enough to cause a departure from the fully reversible case as given in Figs. 2 and 3. In Fig. 6 there is no difference between the substrate fluxes for the hybrid electrode and the *esm* curves, even though the reverse peak is greatly diminished due to the chemical step. However, Fig. 7 indicates that the average concentration distribution at the hybrid electrode (i.e. curve (c)) does not coincide with the substrate concentration of the *equivalent sphericity model*.

For this mechanism, the surface flux of the substrate is equal to the sum of the fluxes of both the product and its subsequent transformed state, Y, if they all have the same diffusivities. Conservation of mass and the reversibility of the electron transfer ensure that these fluxes are independent of spatial considerations. However, the increased efficiency of transport to a spherical electrode as the radius is decreased influences the surface concentration of the substrate as demonstrated in Fig. 7. The concentration dispersion created by having two different degrees of sphericity on either side of the support prevent the hybrid electrode being adequately described by the simplified *equivalent sphericity model*.

Conclusion

From an experimental perspective it is surprising that the powerful observations of Vieil and co-workers have not been more widely adopted especially with the increase in the range of electrode geometries that are currently being used. Although we have only considered diffusive transport here, Vieil's demonstration using a rotating disk electrode under unknown hydrodynamic conditions where a tractable mathematical description was unavailable, shows how important the role of uniform accessibility is in simplifying the theoretical analysis. In Vieil's case the convective component of the transport ensured that the surface concentration of the substrate was uniform across the majority of the electrode surface and this enabled various useful convolutions to be performed during the analysis procedure.

In general, the analysis of a straightforward electrode model has clearly demonstrated that the conditions described in the three previously proposed conditions do lead to a situation where uniform surface concentrations prevail and the convolutions described by Eqs. (2) and (3) can be applied. In all other cases, the spatial distribution of the surface concentrations across an electrode surface must be explicitly considered. This is especially significant when slow electron transfer is apparent.

Acknowledgements A RSC Fellowship from the Research School of Chemistry at the Australian National University is gratefully acknowledged, as is the financial support of the Natural Sciences and Engineering Research Council of Canada.

References

1. Brydon GA, Oldham KB (1981) J Electroanal Chem 122:353
2. Oldham KB (1981) J Electroanal Chem 122:1
3. Goodisman J (1983) J Electroanal Chem 144:33
4. Myland JC, Oldham KB (1983) J Electroanal Chem 147:295
5. Nyholm L, Wikmark G (1987) Anal Chem 59:2383
6. Fleischmann M, Pons S, Rolison DR, Schmidt PP (1987) Ultramicroelectrodes. Datatech Systems Inc., Morganton
7. Molina A, Serna C, Lopeztenes M (1990) J Electroanal Chem 284:21
8. Galvez J, Alcaraz ML, Shim YB, Park SM (1992) J Electroanal Chem 341:15
9. Galvez J, Schroder KH (1993) J Electroanal Chem 361:121
10. Cope DK, Tallman DE (1994) J Electroanal Chem 373:53
11. Cope DK (1997) J Electroanal Chem 439:7
12. Wightman RM, Wipf DO (1989) Electroanal Chem 15:267
13. Bond AM (1994) Analyst 119:R1
14. Amatore C, Maisonhaute E, Simonneau G (2000) Electrochem Commun 2:81
15. Amatore C, Bouret Y, Maisonhaute E, Abruna HD, Goldsmith JI (2003) C R Chim 6:99
16. Bond AM, Oldham KB, Zoski CG (1989) Anal Chim Acta 216:177
17. Zoski CG (1990) J Electroanal Chem 296:317
18. Fletcher S, Horne MD (1999) Electrochem Commun 1:502
19. Schwarz J, Kaden H, Enseleit U (2000) Electrochem Commun 2:606
20. Davies TJ, Ward-Jones S, Banks CE, del Campo J, Mas R, Munoz FX, Compton RG (2005) J Electroanal Chem 585:51
21. Davies TJ, Compton RG (2005) J Electroanal Chem 585:63
22. Vieil E (1991) J Electroanal Chem 297:61
23. Vieil E (1994) J Electroanal Chem 364:9
24. Miomandre F, Vieil E (1994) J Electroanal Chem 375:275
25. Vieil E, Miomandre F (1995) J Electroanal Chem 395:15
26. Vieil E, Lopez C (1999) J Electroanal Chem 466:218
27. Mahon PJ, Oldham KB (2001) Electrochim Acta 46:953

[3]The values of k_f and k_b at the standard potential, E^o, are equal to k^o, the standard heterogeneous rate constant.

28. Mahon PJ, Myland JC, Oldham KB (2002) J Electroanal Chem 537:1
29. Mahon PJ, Oldham KB (1999) J Electroanal Chem 464:1
30. Mahon PJ, Oldham KB (2004) Electrochim Acta 49:5049
31. Oldham KB (1986) Anal Chem 58:2296
32. Zoski CG, Oldham KB, Mahon PJ, Henderson TLE, Bond AM (1991) J Electroanal Chem 297:1
33. Bond AM, Mahon PJ, Maxwell EA, Oldham KB, Zoski CG (1994) J Electroanal Chem 370:1
34. Mahon PJ, Oldham KB (1998) J Electroanal Chem 445:179
35. Rudolph M, Reddy DP, Feldberg SW (1994) Anal Chem 66:589A
36. Oldham KB (1991) J Electroanal Chem 297:317
37. Bard AJ, Faulkner LR (1980) Electrochemical methods: fundamentals and application, Wiley, New York
38. Bowyer WJ, Engelman EE, Evans DH (1989) J Electroanal Chem 262:67
39. Amatore C, Maisonhaute E, Simonneau G (2000) J Electroanal Chem 486:141